On the Effect of the BSSE on Intermolecular Potential Energy Surfaces. Comparison of *a priori* and *a posteriori* BSSE Correction Schemes

PEDRO SALVADOR,[1,2] BÉLA PAIZS,[1,*] MIQUEL DURAN,[2] SÁNDOR SUHAI[1]

[1]*Department of Molecular Biophysics, German Cancer Research Center, Im Neuenheimer Feld 280, D-69120 Heidelberg, Germany*

[2]*Institut de Química Computacional i Departament de Química, Universitat de Girona, 17071, Girona (Catalonia), Spain*

Received 1 November 2000; accepted 12 December 2000

ABSTRACT: A comparative study of geometrical parameters is performed on the complexes HF–HF, H_2O–H_2O, and HF–H_2O using 12 different basis sets at the RHF, MP2, and DFT (BLYP and B3LYP) levels of theory. The equilibrium geometries were obtained from uncorrected, *a posteriori* (counterpoise, CP) and *a priori* (Chemical Hamiltonian Approach, CHA) BSSE-corrected potential energy surfaces. The calculation of equilibrium geometries using the CP and CHA schemes is described in details. The effect of the BSSE on various intermolecular parameters is discussed and the performance of the applied theoretical models is critically evaluated from the BSSE point of view. J Comput Chem 22: 765–786, 2001

Keywords: intermolecular complex; ab initio; geometry optimization; BSSE; CP-scheme; CHA

Introduction

Calculations of the structure of molecular complexes are a challenge for a computational chemist. Beside the usual questions of quantum chemistry (e.g., which basis set to be used at which level of theory), one has to face the problem of the Basis Set Superposition Error (BSSE). The BSSE is a mathematical artifact, and is due to the fact that practical quantum chemical calculations are restricted to the use of finite basis sets. In such a situation, the whole basis set corresponding to the supermolecule is used to describe "internal" properties of the monomers. Because the BSSE is strongly geometry dependent, the corresponding potential energy surfaces can substantially differ from the BSSE-free ones.

Correspondence to: B. Paizs; e-mail: B.Paizs@dkfz.de

*Permanent address: Institute of Chemistry, Hungarian Academy of Sciences, P.O. Box 17, 1525 Budapest, Hungary

The usual way to correct for BSSE is based on the *a posteriori* Boys–Bernardi[1] (counterpoise, CP) scheme. Using the CP scheme one has to recalculate the monomers in the basis of the whole supermolecule for every geometrical arrangement. For example, in the case of two interacting monomers, the uncorrected interaction energy (ΔE) can be calculated as

$$\Delta E = E_{AB}(AB) - E_A(A) - E_B(B), \tag{1}$$

where $E_{AB}(AB)$ is the total energy of the complex, and $E_A(A)$ and $E_B(B)$ are the energies of the monomers calculated in the respective monomer basis sets. (In the following we will use subscripts to denote the molecular species in energy formulas, the patterns in parentheses refer to which basis was used in the calculation. For example, $E_A(A)$ is the energy of monomer A calculated by using its own basis set only.) The CP-corrected interaction energy can be defined as

$$\Delta E^{CP} = E_{AB}(AB) - E_A(AB) - E_B(AB), \tag{2}$$

where $E_A(AB)$ and $E_B(AB)$ are the energies of the monomers calculated in the whole supermolecule basis. Using eqs. (1) and (2), one can define the BSSE content of the interaction energy as

$$\begin{aligned}\delta^{BSSE} &= \Delta E - \Delta E^{CP} \\ &= E_A(AB) - E_A(A) + E_B(AB) - E_B(B).\end{aligned} \tag{3}$$

Using eq. (3) one can define the CP corrected potential energy surface (PES) of a dimer as

$$\begin{aligned}E^{CP} &= E_{AB}(AB) - \delta^{BSSE} \\ &= E_{AB}(AB) + E_A(A) - E_A(AB) \\ &\quad + E_B(B) - E_B(AB).\end{aligned} \tag{4}$$

Note that, whereas the definition of the CP-corrected interaction energy involve only the so-called dimer-centered basis set (DCBS), to obtain the respective CP-corrected supermolecule description, terms involving both the monomer-centered basis set (MCBS) and DCBS are necessary. This is due to the fact that, when the goal is to obtain a correct description of the supermolecule, their fragments can not be frozen at their isolated geometries. Thus, according to eq. (4), one has to calculate five different total energies[2] at every geometrical arrangement of the system to determine a CP-corrected PES. Of course, eq. (4) can be generalized to the case of an arbitrary number of subsystems, but the number of energy calculations necessary to determine the PES increases with the number of monomers in an enormous manner.[3] As Simon, Duran, and Dannenberg[4] have showed recently, various derivatives of eq. (4) can easily be calculated. For example, the gradient on the CP-corrected surface can be calculated as

$$\begin{aligned}\frac{\partial E^{CP}}{\partial x} &= \frac{\partial E_{AB}(AB)}{\partial x} + \frac{\partial E_A(A)}{\partial x} - \frac{\partial E_A(AB)}{\partial x} \\ &\quad + \frac{\partial E_B(B)}{\partial x} - \frac{\partial E_B(AB)}{\partial x},\end{aligned} \tag{5}$$

where x is a geometry parameter. Simon, Duran, and Dannenberg[4] have implemented UNIX scripts and small FORTRAN programs to organize the calculation of such derivatives (gradients, Hessians). Using their program system they were able to determine CP-corrected structures of small hydrogen-bonded complexes and to evaluate the effect of the BSSE on various inter- and intramolecular properties like geometries, vibrational frequencies, and X–H frequency shifts.

A conceptually different way to handle BSSE is to apply the "Chemical Hamiltonian Approach" (CHA)[5] for the case of intermolecular complexes. (For an excellent recent review on CHA, see ref. 6.) CHA eliminates the nonphysical terms of the Hamiltonian that are due to BSSE. By using the *a priori* CHA method one can predict various BSSE-free quantities like one-electron properties derived from BSSE-free wave functions, geometries, etc. Therefore, the main difference between the CHA and the CP approaches is that while CP is a correction method to the energy and its derivatives, CHA is a BSSE-free model of the supermolecule. Because a recent review[6] on CHA is available, here we discuss only those aspects of CHA that are important from the CHA PES point of view. In the CHA framework, the Hamiltonian ($\hat{H}$) can be decomposed by means of a mixed fomulation of the second quantization for nonorthogonal orbitals as

$$\hat{H} = \hat{H}^{Phys} + \hat{H}^{BSSE}, \tag{6}$$

where $\hat{H}^{Phys}$ and $\hat{H}^{BSSE}$ refer to the physical and BSSE terms of the Hamiltonian, respectively. The $\hat{H}^{Phys}$ contains the pure intermolecular interaction terms as well as the sum of the effective monomer Hamiltonians.[6] The BSSE-type terms collected in $\hat{H}^{BSSE}$ arise from the difference between the conventional and effective monomer Hamiltonians.

At various levels of CHA, $\hat{H}^{Phys}$ is used to define theoretical models in conjunction with the applied wave function. For example, one can derive SCF-type CHA equations based on $\hat{H}^{Phys}$ and an one-determinantal wave function.

One of the typical aspects of CHA is that the total energy is calculated as an expectation value of the full Hamiltonian over the CHA wave

function[6] (Ψ^{CHA}):

$$E^{CHA} = \frac{\langle \Psi^{CHA} | \hat{H} | \Psi^{CHA} \rangle}{\langle \Psi^{CHA} | \Psi^{CHA} \rangle}. \quad (7)$$

Equation (7) defines the BSSE-free CHA potential energy surface for the supermolecule. One of the advantages of CHA over the CP scheme is that in the former case the BSSE-free PES can be determined by a single energy calculation for every geometrical arrangement of the system. However, derivatives of eq. (7) involve the solution of the CHA version[7] of the coupled-perturbed Hartree–Fock (CPHF) equations.[8] One has to determine the gradient of the SCF coefficients (C_i) with respect to the geometry parameters (x). Once the partial derivatives $\partial C_i/\partial x$ are known, calculation of the CHA–SCF gradient is straightforward.[9] However, the calculation of the derivatives of the SCF parameters is a rather time-consuming procedure. First, the CHA CPHF equations have to be solved for all the geometrical parameters. Second, the solution of the CHA CPHF equations does involve a full SCF-type procedure making the practical calculation of the CHA gradient insufficient from the computational point of view. Because the CHA models are not based on variational methods, it is obvious to apply techniques that make the calculation of gradients of nonvariational correlation methods (Mp*n*, Coupled Cluster) efficient. These techniques are based on the so-called Z-vector method[10] or algorithms that use fully variational correlation functionals instead of the traditional nonvariational ones.[11] The application of such techniques is possible in the CHA framework, but the CHA–SCF gradient formulas based on the Z-vector or on fully variational methods are still too complicate for practical computations at the SCF level of theory.[9] One has to mention that this fact does not hold for the recently developed CHA–MP2 method.[12] Here, the cost of the gradient calculation seems to be comparable to that of the energy determination. The work on developing gradient techniques at various CHA levels is in progress in our laboratory.

In this study, we have used the so-called CHA/F version of the Chemical Hamiltonian Approach. Within this formulation the correction of BSSE is performed to the Fockian matrix, instead to the Hamiltonian, which allows to apply in a straightforward way the CHA at the Density Functional (DFT) level of theory.

Beside the special BSSE problems in the intermolecular framework, there are some other questions to be addressed. The final goal is to set up models (computational strategies) that can predict various parameters that are close to the experimental values when the later is available. One way to achieve this task is to calculate intermolecular complexes in a very accurate manner. This involves the use of correlation methods (MP*n*, CC) in conjunction with large basis sets. Because it is nearly impossible to reach the basis set limit in these calculations, the determination of various properties on the BSSE-corrected PES seems to be mandatory. Furthermore, to calculate accurate energy differences correction for zero-point energy (ZPE) is rather important. Calculation of thermal energy corrections is also based on frequency calculations. To achieve accurate thermochemical data the frequency calculations should be corrected for anharmonicity. From the previous list of problems to be solved it is clear that this way of hunting for chemical accuracy in the intermolecular framework is not a trivial task. Another possibility to obtain reasonable results is to apply a model (strategy) that is simpler than the one described above but its accuracy is still close to that required in chemical applications. Of course, this situation can occur only if the errors arising from the neglected features of the sophisticated approach mentioned above cancel each other. A very promising theoretical model from this point of view is the MP2/6-31+G(d,p) method widely used by Del Bene and coworkers.[13] These authors calculated various properties (geometry, interaction energy, frequencies, and X–H frequency shifts) of intermolecular complexes ranging from hydrogen bonded to Van der Waals systems, and found that the MP2/6-31+G(d,p) results are quite reasonable. Good agreement with experimental results was achieved despite the fact that only a moderate basis set was used in the calculations, the correlation expansion was truncated at the MP2 level, the geometries were obtained from a PES containing BSSE, and anharmonicity was not considered in the frequency calculations. In our opinion, the MP2/6-31+G(d,p) theoretical model is a fortunate choice for such calculations, because the various errors present in the model reasonably cancel each other. Of course, application of such an error balanced method is not the safest choice, but the range of molecular systems that can be reached in this way is wider than that of the error-free approach described above.

In the present article we address the problems of intermolecular structure determination described above. One of the most important questions is how the BSSE distort the calculated PES and how the *a posteriori* and *a priori* BSSE correction schemes perform compared to each other. To evaluate these

problems we carried out gradient optimizations for the HF–HF, H_2O–H_2O, and H_2O–HF complexes at the SCF, DFT, and MP2 levels of theory in conjunction with 12 different basis sets of increasing size. Analogous calculations were performed using both the counterpoise (CP–SCF, CP–DFT and CP–MP2) and the CHA (CHA/F–SCF and CHA/F–DFT) BSSE correction schemes. Geometry parameters and interaction energies were determined for the by using all the possible theoretical models that can be derived from the sets of methods and basis functions listed above. We chose these complexes because accurate experimental results are available and it is well known that DFT methods predict quite reasonable results for these particular cases.[14] From the analysis of the data calculated as described above we expect that some of the questions listed in the first part of this chapter can be answered.

Computational Details

All the *ab initio* calculations were carried out using the Gaussian-92[18] and Gaussian-94[19] program systems. For the CHA/F computations we used our modified version of Gaussian-92.[20] For the CHA/F geometry optimizations the gradients were determined by the finite difference method. For the CP geometry optimizations we used the program system described in ref. 4 with some small modifications in both the scripts and various Gaussian links. For the calculations Pople's 6-31G, 6-31G(d), 6-31G(d,p), 6-31++G(d,p), 6-311G(d,p), 6-311++G(d,p), 6-311++G(2df,2p), and 6-311++G(3df,2pd) and Dunning's TZV(d,p), TZV(d,p)++, aug-cc-pVDZ, and aug-cc-pVTZ basis sets were used. In the DFT calculations the BLYP (Becke exchange[21] and Lee, Yang, Parr correlation[22]) and B3LYP (Becke's three parameter exchange[23] and Lee, Yang, Parr correlation[22]) potentials were applied.

Results

HF DIMER

The HF dimer has a linear structure that is known from both experiment[24, 28] and high-level calculations.[25, 26] However, it is also well known[13, 27] that DFT methods in conjunction with small basis sets tend to predict the cyclic structure to be the only stable one on the PES. In the following, both these pathological and the linear cases will be examined from the point of view of BSSE. Tables I and II summarize selected geometrical parameters of the HF dimer (Fig. 1) calculated at the uncorrected and corrected SCF, BLYP, B3LYP, and MP2 levels of theory using the Pople and the TZP** and TZP++** basis sets. The corresponding interaction energies are shown graphically in Figure 2. The dependence of the distance between the fluorine atoms on the applied theoretical model is also shown graphically in Figure 3.

Concerning the effect of the BSSE on the energetics and geometry of the HF dimer, the following conclusions can be drawn. In all cases part of the binding is due to the BSSE, the uncorrected interaction energies are always larger than the corrected ones. The corrected intermolecular distances (*rff*, the distance between the fluorine atoms) are always longer than the corresponding uncorrected values. This finding is in line with literature data.[4, 6] The difference between the uncorrected and corrected *rff* distances is rather large in the case of small basis sets but gets smaller by using larger basis sets. Analyzing the data presented in Tables I and II it can be seen that even in the case of the 6-311++G(3df,2pd) basis set the corrected and uncorrected *rff* distances differ from each other by 0.015–0.025, 0.005–0.015, and 0.044–0.055 Å at the SCF, DFT, and MP2 levels, respectively. Except for a few cases when the optimization leads to distorted structures, the uncorrected SCF *rff* distances are longer than the corresponding experimental[24] value of 2.72 Å. Correction for BSSE even lengthens these distances; the corrected parameters are farther from the experimental value than the uncorrected ones. Disregarding the pathological cases discussed below in detail, DFT methods predict reasonable *rff* distances especially in the case of the B3LYP fuctional. The BSSE has an enormous effect on the *rff* distances determined from MP2 calculations. The uncorrected *rff* values are close to the experimental data. The CP corrected MP2 *rff* distances are always larger than the experimental value; the difference between the corrected and uncorrected MP2/6-311++G(3df,2pd) distances is still 0.044 Å. These results show that BSSE effects are significant in the MP2 calculations even using the largest Pople basis sets.

Furthermore, the BSSE can have smaller or larger effect on the intermolecular bond angles. This effect is quite large using the SCF method in conjunction with small basis sets, and results highly distorted uncorrected structures. In these cases correction for the BSSE leads to reasonable geometrical parameters. By the appearance of diffuse functions the

TABLE I.
Geometrical Parameters for the HF–HF Dimer Calculated in 10 Different Basis Sets as the SCF, CHA/F-SCF, CP-SCF, MP2, and CP-MP2 Levels of Theory.

Basis Set	Method	*rff* (≈)	α	β	Method	*rff* (≈)	α	β
6-31G	SCF	2.706	8.3	126.0	MP2	2.719	12.5	109.0
(22)	CHA/F-SCF	2.713	5.1	135.6	CP-MP2	2.789	4.5	133.8
	CP-SCF	2.741	3.7	143.1				
6-31G*	SCF	2.709	17.1	96.6	MP2	2.535	45.3	51.8
(34)	CHA/F-SCF	2.756	7.6	114.8	CP-MP2	2.790	6.5	113.7
	CP-SCF	2.798	6.9	117.7				
6-31G**	SCF	2.725	14.4	101.7	MP2	2.541	47.8	48.9
(40)	CHA/F-SCF	2.760	8.3	116.7	CP-MP2	2.799	6.6	115.2
	CP-SCF	2.811	6.7	120.1				
6-31++G**	SCF	2.812	8.0	120.0	MP2	2.776	7.6	115.3
(50)	CHA/F-SCF	2.831	7.4	120.8	CP-MP2	2.836	7.7	114.9
	CP-SCF	2.842	7.5	120.8				
6-311G**	SCF	2.773	11.6	112.6	MP2	2.710	17.8	94.7
(50)	CHA/F-SCF	2.822	7.7	122.8	CP-MP2	2.850	6.0	121.9
	CP-SCF	2.850	6.3	126.3				
6-311++G**	SCF	2.825	6.4	126.7	MP2	2.791	6.6	120.9
(60)	CHA/F-SCF	2.868	6.8	126.3	CP-MP2	2.880	7.3	120.6
	CP-SCF	2.871	7.0	126.4				
TZV**	SCF	2.796	5.9	128.1	MP2	2.756	5.6	122.8
(52)	CHA/F-SCF	2.824	5.7	129.4	CP-MP2	2.842	5.5	124.9
	CP-SCF	2.827	5.7	129.9				
TZV++**	SCF	2.809	5.9	129.5	MP2	2.782	5.6	125.1
(62)	CHA/F-SCF	2.829	6.6	127.9	CP-MP2	2.851	7.4	121.8
	CP-SCF	2.833	6.8	128.0				
6-311++G(2df,2p)	SCF	2.837	7.6	120.4	MP2	2.762	7.7	111.0
(98)	CHA/F-SCF	2.851	7.9	120.5	CP-MP2	2.817	7.7	113.5
	CP-SCF	2.860	7.8	120.8				
6-311++G(3df,2pd)	SCF	2.821	7.0	118.7	MP2	2.749	6.5	112.2
(122)	CHA/F-SCF	2.840	7.2	119.9	CP-MP2	2.793	7.1	112.2
	CP-SCF	2.846	7.1	119.9				

The number of basis functions is given in parentheses. The experimental[24] values of *rff* (r_e), α, and β are ≈2.72, 10±6°, and 117±6°, respectively. For notation, see Figure 1.

corrected and uncorrected bond angles get very close to each other. In the case of the correlation methods, the differences between the corrected and uncorrected bond angles are larger than the corresponding SCF values even if we do not consider the totally pathological cases that will be discussed later in detail. In the case of the largest Pople basis sets the corrected bond angles can still differ from the uncorrected ones by a few degrees. It is to be noted in this respect that one cannot find any tendency even in the case of the CP or CHA surfaces regarding the anisotropy of the PES. Basis set effects are rather important as well; however, it is not easy to justify which theoretical model is preferable in this respect because of the large uncertainties of the experimental results. Because the intramolecular parameters (F–H distances) are not affected by the BSSE, their actual values are not reported so as to save space.

Comparing the behavior of the *a priori* and *a posteriori* correction schemes, one can find larger differences when small or moderate basis sets are used in the computations. By comparing CP and CHA results one can explore the adequacy of the basis sets in a given computational situation.

Except for a few cases when the CP and CHA values are very close to each other, the CP intermolecular distances (*rff*) are longer than the correspond-

TABLE II.

Geometrical Parameters for the HF–HF Dimer Calculated in 10 Different Basis Sets as the BLYP, CHA/F-BLYP, CP-BLYP, B3LYP, CHA/F-B3LYP, and CP-B3LYP Levels of Theory.

Basis Set	Method	*rff* (≈)	α	β	Method	*rff* (≈)	α	β
6-31G	BLYP	2.480	46.7	47.2	B3LYP	2.478	48.5	49.8
(22)	CHA/F-BLYP	2.662	5.6	114.9	CHA/F-B3LYP	2.647	5.2	120.0
	CP-BLYP	2.735	5.4	120.1	CP-B3LYP	2.701	4.7	125.2
6-31G*	BLYP	2.485	44.9	45.2	B3LYP	2.485	46.0	47.0
(34)	CHA/F-BLYP	2.652	5.2	105.9	CHA/F-B3LYP	2.647	5.7	107.5
	CP-BLYP	2.762	7.1	107.0	CP-B3LYP	2.732	6.8	109.5
6-31G**	BLYP	2.494	44.9	44.9	B3LYP	2.493	46.0	46.9
(40)	CHA/F-BLYP	2.626	7.6	105.2	CHA/F-B3LYP	2.627	7.8	107.5
	CP-BLYP	2.781	7.2	108.7	CP-B3LYP	2.749	7.0	111.3
6-31++G**	BLYP	2.760	7.5	111.6	B3LYP	2.732	7.6	113.1
(50)	CHA/F-BLYP	2.782	7.4	110.6	CHA/F-B3LYP	2.752	7.4	112.5
	CP-BLYP	2.786	7.8	109.9	CP-B3LYP	2.758	7.7	112.0
6-311G**	BLYP	2.572	46.9	48.3	B3LYP	2.567	47.2	51.2
(50)	CHA/F-BLYP	2.730	8.8	107.9	CHA/F-B3LYP	2.725	7.0	113.9
	CP-BLYP	2.809	7.2	113.6	CP-B3LYP	2.777	6.9	116.3
6-311++G**	BLYP	2.778	6.9	116.2	B3LYP	2.747	7.3	117.5
(60)	CHA/F-BLYP	2.822	6.3	115.6	CHA/F-B3LYP	2.790	7.0	116.9
	CP-BLYP	2.816	8.0	113.1	CP-B3LYP	2.785	7.9	115.5
TZV**	BLYP	2.740	6.6	115.4	B3LYP	2.716	6.5	117.8
(52)	CHA/F-BLYP	2.783	6.1	116.5	CHA/F-B3LYP	2.751	6.2	118.8
	CP-BLYP	2.786	6.5	116.5	CP-B3LYP	2.756	6.4	119.0
TZV++**	BLYP	2.764	7.2	117.1	B3LYP	2.734	7.2	119.1
(62)	CHA/F-BLYP	2.787	6.4	116.0	CHA/F-B3LYP	2.755	6.7	117.9
	CP-BLYP	2.786	7.8	114.1	CP-B3LYP	2.755	7.7	116.7
6-311++G(2df,2p)	BLYP	2.775	9.0	107.0	B3LYP	2.750	8.1	111.0
(98)	CHA/F-BLYP	2.784	8.4	107.5	CHA/F-B3LYP	2.756	6.0	113.7
	CP-BLYP	2.790	7.7	108.9	CP-B3LYP	2.760	7.8	110.9
6-311++G(3df,2pd)	BLYP	2.768	5.3	112.0	B3LYP	2.734	5.8	112.5
(122)	CHA/F-BLYP	2.778	4.8	113.0	CHA/F-B3LYP	2.747	5.4	113.9
	CP-BLYP	2.780	6.9	109.1	CP-B3LYP	2.750	7.0	110.9

The number of basis functions is given in parentheses. The experimental[24] values of *rff* (r_e), α, and β are ≈2.72, 10±6°, and 117±6°, respectively. For notation, see Figure 1.

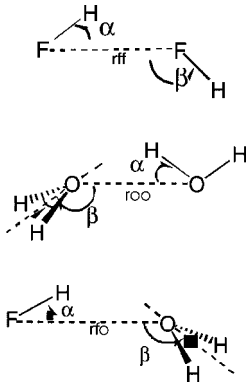

FIGURE 1. Geometrical parameters of the $(HF)_2$, $(H_2O)_2$, and $HF–H_2O$ complexes.

ing CHA values. In the case of small basis sets, the difference between the CP and CHA values can be rather large (e.g., 0.105 Å at the B3LYP/6-31G(d) level of theory), but the difference gets smaller as the applied basis set is improved. From this point of view the role of diffuse functions is rather important, by their appearance the difference between the CP and CHA corrected *rff* values gets close to 0.005 Å. The largest deviations between the CP and CHA corrected *rff* values can be found in those cases when the uncorrected model fails to describe even qualitatively the PES of the HF dimer.

As we mentioned above, the DFT methods in conjunction with small basis sets tend to predict the

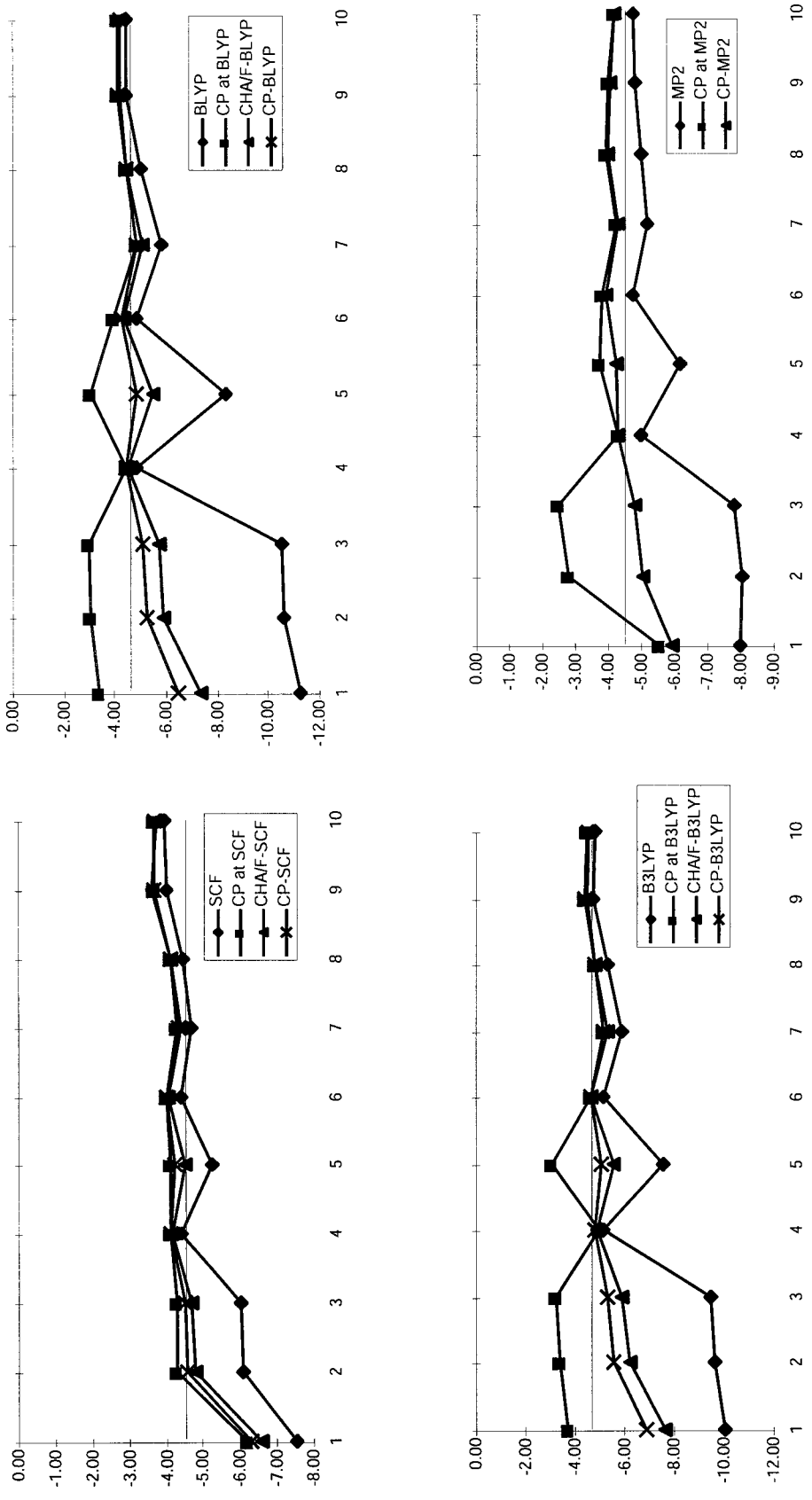

FIGURE 2. Electronic interaction energy (kcal/mol) for the complex $(HF)_2$ in 10 basis sets. Basis sets are: (1) 6-31G, (2) 6-31G(d), (3) 6-31G(d,p), (4) 6-31++G(d,p), (5) 6-311G(d,p), (6) 6-311++G(d,p), (7) TZV(d,p), (8) TZV++(d,p), (9) 6-311++G(2df,2p), and (10) 6-311++G(3df,2pd). The experimental[30] interactions energy is -4.56 ± 0.29 kcal/mol (horizontal solid line).

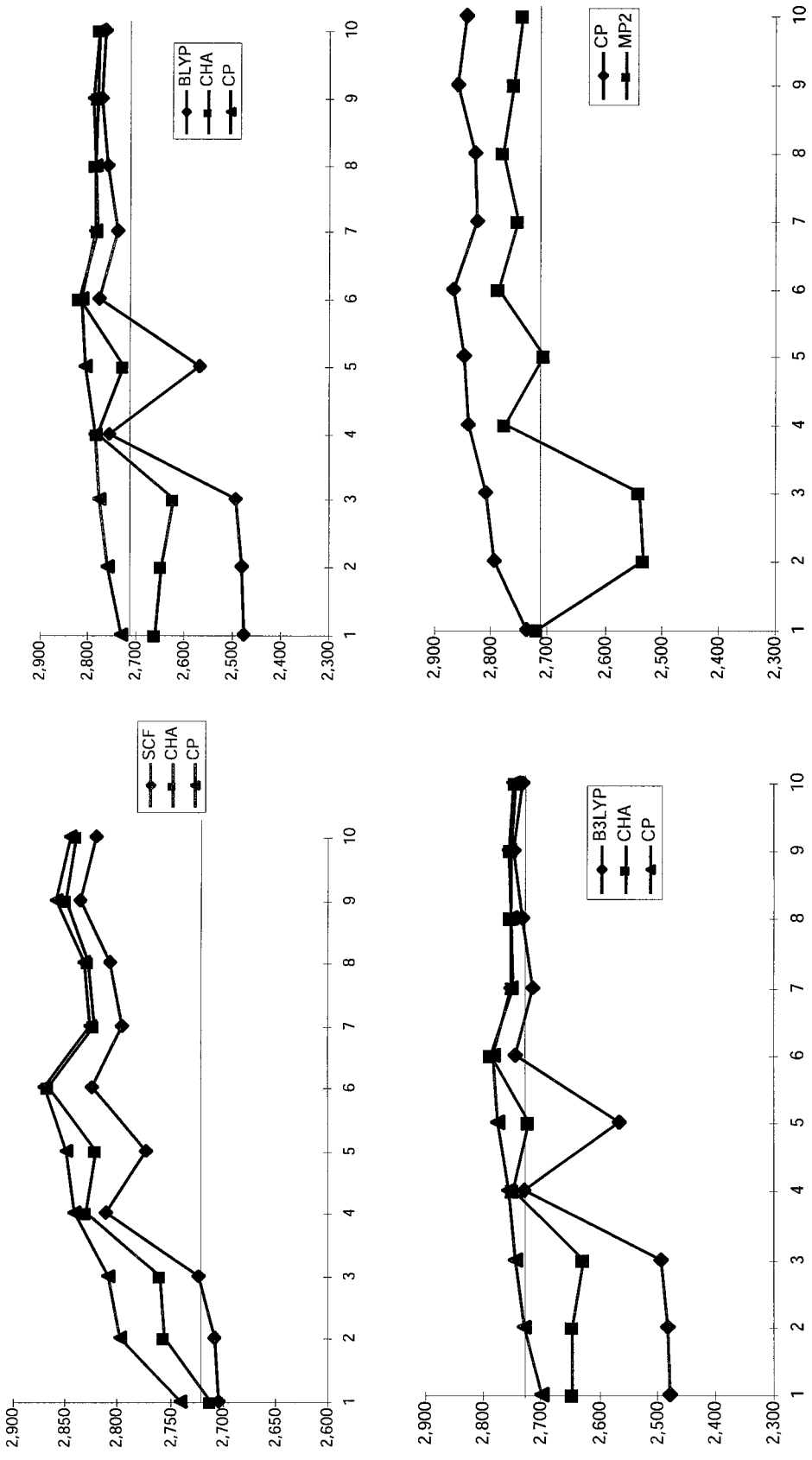

FIGURE 3. Distance between flourine atoms for the complex $(HF)_2$ in 10 basis sets. Basis sets are: (1) 6-31G, (2) 6-31G(d), (3) 6-31G(d,p), (4) 6-31++G(d,p), (5) 6-311G(d,p), (6) 6-311++G(d,p), (7) TZV(d,p), (8) TZV++(d,p), (9) 6-311++G(2df,2p), and (10) 6-311++G(3df,2pd). The experimental[26] *rff* distance is ≈2.72 (horizontal solid line).

cyclic structure to be the only stable one on the PES of the HF dimer. These pitfalls of the DFT methods can be seen also in our results in the case of the 6-31G, 6-31G(d), 6-31G(d,p), and even 6-311G(d,p) basis sets. Here, the α and β bond angles are close to 45°, and the *rff* distance is shorter than the corresponding experimental value of 2.72 Å. On the other hand, both the CHA and the CP optimization lead to the bent structure, in these cases correcting the pitfall of the underlying uncorrected models. One has to note in this respect that this behavior described above is believed in the literature as a problem of DFT methods. However, optimizations at the MP2/6-31G(d) and MP2/6-31G(d,p), levels also lead to the cyclic structure, while the MP2/6-31G and MP2/6-311G(d,p) models predict distorted bent structures. Optimizations on the corresponding CP-corrected potential energy surfaces lead to the bent structure, and predict [except for MP2/6-31G(d)] reasonable bond angles.

One can calculate the interaction energy of an intermolecular complex considering both BSSE and geometry effects in a few ways. First, the interaction energy can be calculated after geometry optimization of the complex without any correction for BSSE. Second, one can calculate the BSSE-corrected interaction energy at the optimized geometry. Furthermore, one can correct (CP or CHA) for the BSSE during the geometry optimization also, and determine BSSE-corrected interaction energies using geometries obtained from BSSE-free potential energy surfaces. In Figure 2 we show our results for the interaction energy of the HF dimer obtained by using the four procedures described above. The behavior of the first two procedures is not satisfactory. Calculations without any BSSE correction can lead to high interaction energies while single point CP corrections at the final (uncorrected) geometries can predict too weak interaction for small basis sets. Of course this behavior is due to the tendency that some of the uncorrected DFT and MP2 optimizations lead to the cyclic structure. On the other hand, corrected interaction energies computed at the BSSE-corrected geometries converge fast, independent of whether the CP or CHA method is used in the calculations. It is to be noted that the difference between the CHA and CP interaction energies is always smaller than the difference between the uncorrected and corrected values. Using basis sets with diffuse functions the single point CP-corrected energies get closer to the fully corrected ones. The energy data suggest that it is easier to reach convergence in the interaction energy by improving the quality of the applied basis set than getting close to the limit regarding the surfaces are much flatter than the intramolecular ones. Correction for BSSE seems to be important for both the energy and geometry.

H_2O DIMER

The water dimer (Fig. 1) has a linear structure that is known from both experiment[29] and theoretical calculations.[30] Our geometry results are summarized in Tables III and IV, while the energetics of the water dimer and the dependence of the *roo* distance on the applied theoretical model are shown graphically in Figures 3 and 4, respectively.

Because many of the conclusions drawn in the preceding section are also valid for the water dimer, we do not discuss them in details. Because part of the binding is due to the BSSE, all the corrected intermolecular distances (*roo*) are longer than the corresponding uncorrected ones. The difference between the corrected and uncorrected *roo* distances is similar to those values found in the case of the HF dimer. The SCF *roo* distances are nearly always longer than the corresponding experimental[29] value (2.946 Å), and correction for the BSSE further lengthens this parameter. DFT methods usually underestimate the *roo* distance, the corresponding BSSE-corrected values are closer to experiment (Fig. 5, Table IV). The uncorrected MP2 intermolecular distances are also too short, while the CP-corrected values are usually too large. It is very promising, however, that by improving the quality of the basis both the corrected and uncorrected *roo* distances get close to the experimental value.

Both the BSSE and the quality of the basis set have a large effect on the optimized bond angles. For example, nearly all the optimizations at the SCF level fail to describe the anisotropy of the interaction, in terms of the β angle. The corresponding CP and CHA optimizations do not improve these results. In the case of the DFT methods, the predicted β bond angles are close to the experimental value when one uses the largest basis sets. However, this is not the case for the small and moderate basis sets, but both CP and CHA are able to correct these pitfalls. For example, optimization at the B3LYP/6-31G(d,p) level led to 94.5 degrees, the corresponding CP and CHA values are 114.3 and 119.1 degrees, respectively. The MP2 results also vary on a wide range, one has to use at least moderate size basis sets and corrected models to get reasonable bond angles.

Comparing the behavior of the *a priori* and *a posteriori* correction schemes one can draw similar conclusions as those obtained for the HF dimer. Except for a very few cases the CHA intermolecular

TABLE III.
Geometrical Parameters for the $(H_2O)_2$ Dimer Calculated in 10 Different Basis Sets as the SCF, CHA/F-SCF, CP-SCF, MP2, and CP-MP2 Levels of Theory.

Basis Set	Method	*roo* (≈)	α	β	Method	*roo* (≈)	α	β
6-31G	SCF	2.843	−0.3	152.0	MP2	2.867	2.6	136.8
(26)	CHA/F-SCF	2.866	0.0	155.9	CP-MP2	2.901	0.8	153.2
	CP-SCF	2.862	0.0	157.5				
6-31G*	SCF	2.973	4.6	118.4	MP2	2.916	9.2	101.5
(38)	CHA/F-SCF	2.985	2.6	128.4	CP-MP2	2.978	3.0	126.5
	CP-SCF	3.002	1.4	134.1				
6-31G**	SCF	2.983	5.2	117.3	MP2	2.910	9.8	99.3
(50)	CHA/F-SCF	2.999	2.2	133.1	CP-MP2	2.990	2.8	129.9
	CP-SCF	3.017	1.2	137.2				
6-31++G**	SCF	2.987	2.6	136.2	MP2	2.921	3.5	133.4
(62)	CHA/F-SCF	3.030	1.5	140.6	CP-MP2	3.007	4.6	129.9
	CP-SCF	3.046	1.7	140.2				
6-311G**	SCF	2.975	2.2	129.5	MP2	2.907	4.3	117.0
(62)	CHA/F-SCF	3.036	−0.1	142.8	CP-MP2	3.038	−0.1	140.2
	CP-SCF	3.052	−0.7	146.8				
6-311++G**	SCF	3.000	0.9	142.9	MP2	2.922	2.2	135.7
(74)	CHA/F-SCF	3.048	0.7	146.0	CP-MP2	3.019	3.1	135.7
	CP-SCF	3.049	0.8	146.0				
TZV**	SCF	2.970	2.4	138.2	MP2	2.886	0.0	142.1
(64)	CHA/F-SCF	3.006	0.4	148.9	CP-MP2	2.987	1.6	144.5
	CP-SCF	3.007	0.2	150.3				
TZV++**	SCF	2.976	0.4	147.2	MP2	2.900	1.6	140.2
(76)	CHA/F-SCF	2.996	0.9	148.0	CP-MP2	2.984	3.3	139.5
	CP-SCF	3.006	0.9	148.0				
6-311++G(2df,2p)	SCF	3.039	2.7	134.1	MP2	2.919	4.5	126.2
(118)	CHA/F-SCF	3.056	2.7	137.0	CP-MP2	2.966	5.2	125.7
	CP-SCF	3.060	2.9	136.5				
6-311++G(3df,2pd)	SCF	3.036	2.9	134.2	MP2	2.911	4.8	125.4
(154)	CHA/F-SCF	3.048	2.7	137.3	CP-MP2	2.950	5.3	125.0
	CP-SCF	3.049	3.0	136.4				

The number of basis functions is given in parentheses. The experimental[29] values of *roo*(r_e), α, and β are ≈2.946, 123 ± 10°, and 2 ± 10°, respectively. For notation, see Figure 1.

distances lie between the uncorrected and the CP-corrected ones. Usually, the differences between the CP and CHA intermolecular parameters are smaller than the differences between the corrected and uncorrected values. Larger differences between the *a priori* and *a posteriori* corrected *roo* distances can be found in those cases when the corresponding uncorrected model predicts distorted structures.

Previous studies showed[27] that the linear structures determined at the DFT level with BLYP and B3LYP functionals in conjunction with the 6-31G* and 6-31G** basis sets actually correspond to saddle points. Table IV presents the geometry data calculated at the DFT level with both functionals. It can be seen that both BSSE-free methods correct the rather distorted uncorrected structures, the angular features of these structures are closer to the large basis results than those of the uncorrected ones. We carried out frequency calculations at the corrected and uncorrected BLYP/6-31G(d,p) levels to explore the curvature of the PES from the BSSE point of view. Similarly to the literature data, the Hessian calculated at the uncorrected BLYP/6-31G(d,p) level has a negative eigenvalue. The CHA/DFT(BLYP)

TABLE IV.
Geometrical Parameters for the $(H_2O)_2$ Dimer Calculated in 10 Different Basis Sets as the BLYP, CHA/F-BLYP, CP-BLYP, B3LYP, CHA/F-B3LYP, and CP-B3LYP Levels of Theory.

Basis Set	Method	*roo* (≈)	α	β	Method	*roo* (≈)	α	β
6-31G	BLYP	2.814	6.1	116.0	B3LYP	2.776	3.7	130.2
(26)	CHA/F-BLYP	2.823	4.0	132.1	CHA/F-B3LYP	2.795	3.2	140.5
	CP-BLYP	2.836	2.0	142.2	CP-B3LYP	2.797	1.9	147.7
6-31G*	BLYP	2.868	16.3	82.1	B3LYP	2.861	12.1	93.1
(38)	CHA/F-BLYP	2.896	4.6	111.7	CHA/F-B3LYP	2.878	4.9	114.3
	CP-BLYP	2.941	4.6	115.4	CP-B3LYF	2.911	4.4	119.1
6-31G**	BLYP	2.884	15.2	83.3	B3LYP	2.876	10.9	94.5
(50)	CHA/F-BLYP	2.901	5.5	114.0	CHA/F-B3LYP	2.883	5.6	116.5
	CP-BLYP	2.970	4.5	118.0	CP-B3LYP	2.936	3.9	122.4
6-31++G**	BLYP	2.912	4.2	127.3	B3LYP	2.887	4.2	128.8
(62)	CHA/F-BLYP	2.955	3.5	127.1	CHA/F-B3LYP	2.924	3.7	128.9
	CP-BLYP	2.961	6.2	119.8	CP-B3LYP	2.931	5.7	123.4
6-311G**	BLYP	2.915	7.6	100.5	B3LYP	2.887	8.3	105.1
(62)	CHA/F-BLYP	2.960	2.9	123.2	CHA/F-B3LYP	2.941	2.8	127.3
	CP-BLYP	3.021	1.5	131.1	CP-B3LYP	2.979	1.1	135.3
6-311++G**	BLYP	2.927	3.9	129.5	B3LYP	2.900	3.8	131.3
(74)	CHA/F-BLYP	2.975	3.5	128.3	CHA/F-B3LYP	2.944	3.5	131.1
	CP-BLYP	2.971	5.3	124.8	CP-B3LYP	2.941	4.6	129.5
TZV**	BLYP	2.900	1.7	130.4	B3LYP	2.877	1.0	136.5
(64)	CHA/F-BLYP	2.955	3.7	129.7	CHA/F-B3LYP	2.920	3.7	133.1
	CP-BLYP	2.959	3.6	132.8	CP-B3LYP	2.925	2.9	137.6
TZV++**	BLYP	2.910	3.4	131.2	B3LYP	2.883	2.5	136.1
(76)	CHA/F-BLYP	2.935	3.8	129.7	CHA/F-B3LYP	2.905	3.7	132.4
	CP-BLYP	2.942	5.3	127.2	CP-B3LYP	2.911	4.8	131.3
6-311++G(2df,2p)	BLYP	2.949	5.3	120.4	B3LYP	2.922	4.1	125.9
(118)	CHA/F-BLYP	2.960	5.8	118.4	CHA/F-B3LYP	2.931	4.2	125.6
	CP-BLYP	2.966	6.0	118.7	CP-B3LYP	2.937	5.5	122.3
6-311++G(3df,2pd)	BLYP	2.949	5.7	119.0	B3LYP	2.919	5.1	122.3
(154)	CHA/F-BLYP	2.957	5.7	119.5	CHA/F-B3LYP	2.928	4.0	126.7
	CP-BLYP	2.960	5.7	119.7	CP-B3LYP	2.931	5.2	123.2

The number of basis functions is given in parentheses. The experimental[29] values of *roo*(r_e), α, and β are ≈2.946, $123 \pm 10°$, and $2 \pm 10°$, respectively. For notation, see Figure 1.

optimized structure was characterized as a minimum by calculating the Hessian using numerical derivatives. The adequacy of the numerical differentiation was checked by comparing the accuracy of full numerical and full analytical methods for the case of the uncorrected BLYP/6-31G(d,p) level. Furthermore, analytical CP corrected derivatives were also used to carry out frequency calculation at the CP-corrected structure at the same level.

The CP calculations also result a minimum, so the CP method can also correct the deficiency of the BLYP/6-31G(d,p) model discussed above. Similar calculations were performed for other pathological cases listed above, resulting in the same tendency obtained for the BLYP/6-31G(d,p) model. In the previous chapter we discussed that some of the uncorrected DFT and MP2 models resulted in the cyclic structure of the HF dimer. To check the performance of the MP2 method in the case of the water dimer, we carried out frequency calculations using the 6-31G(d) and 6-31G(d,p) basis sets. Both the MP2/6-31G(d) and MP2/6-31G(d,p) calculations lead to a minimum, indicating that the small basis MP2 models perform better than the corre-

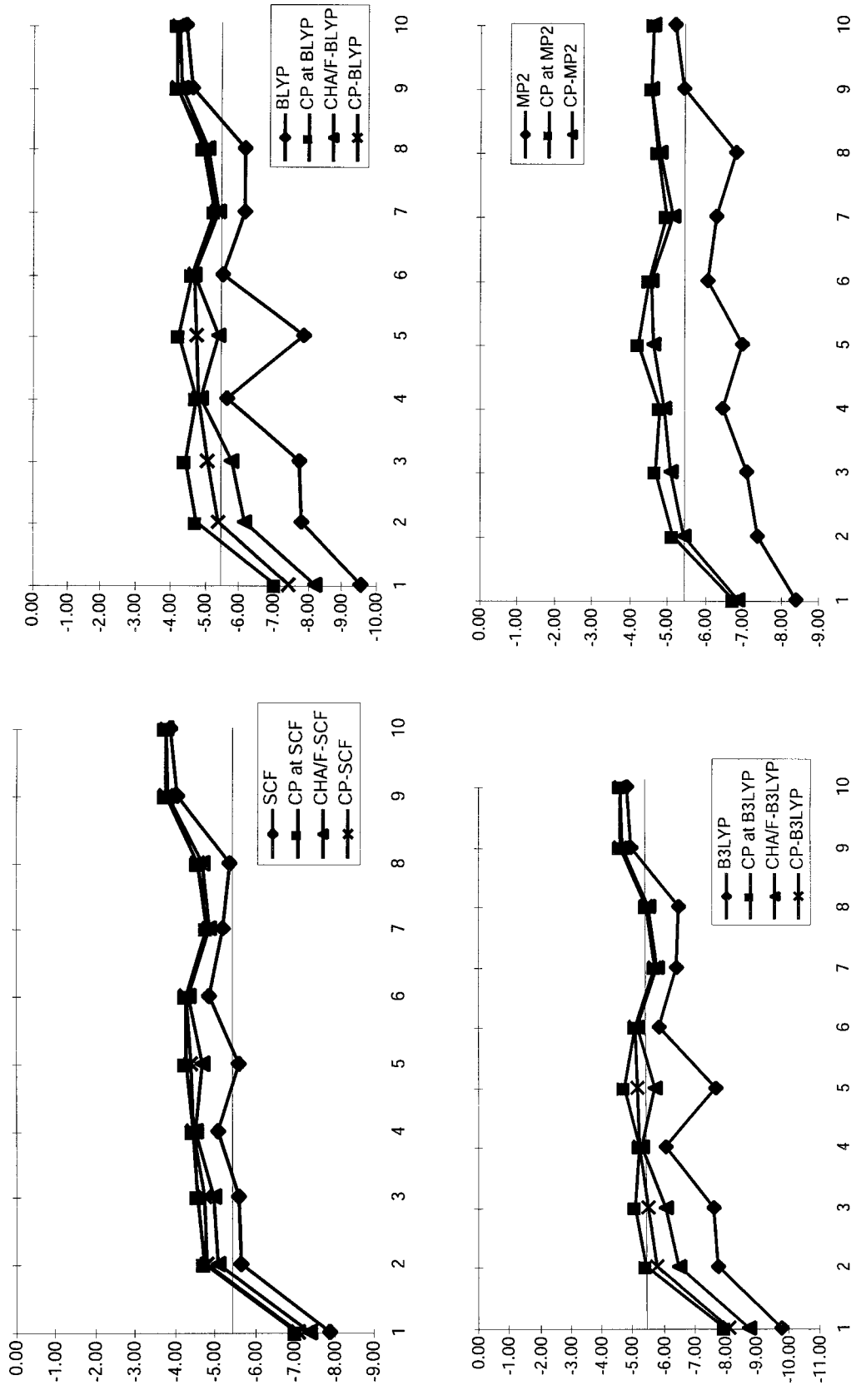

FIGURE 4. Electronic interaction energy (kcal/mol) for the complex $(H_2O)_2$ in 10 basis sets. Basis sets are: (1) 6-31G, (2) 6-31G(d), (3) 6-31G(d,p), (4) 6-31++G(d,p), (5) 6-311G(d,p), (6) 6-311++G(d,p), (7) TZV(d,p), (8) TZV++(d,p), (9) 6-311++G(2df,2p), and (10) 6-311++G(3df,2pd). The experimental[34] interactions energy is -5.4 ± 0.2 kcal/mol (horizontal solid line).

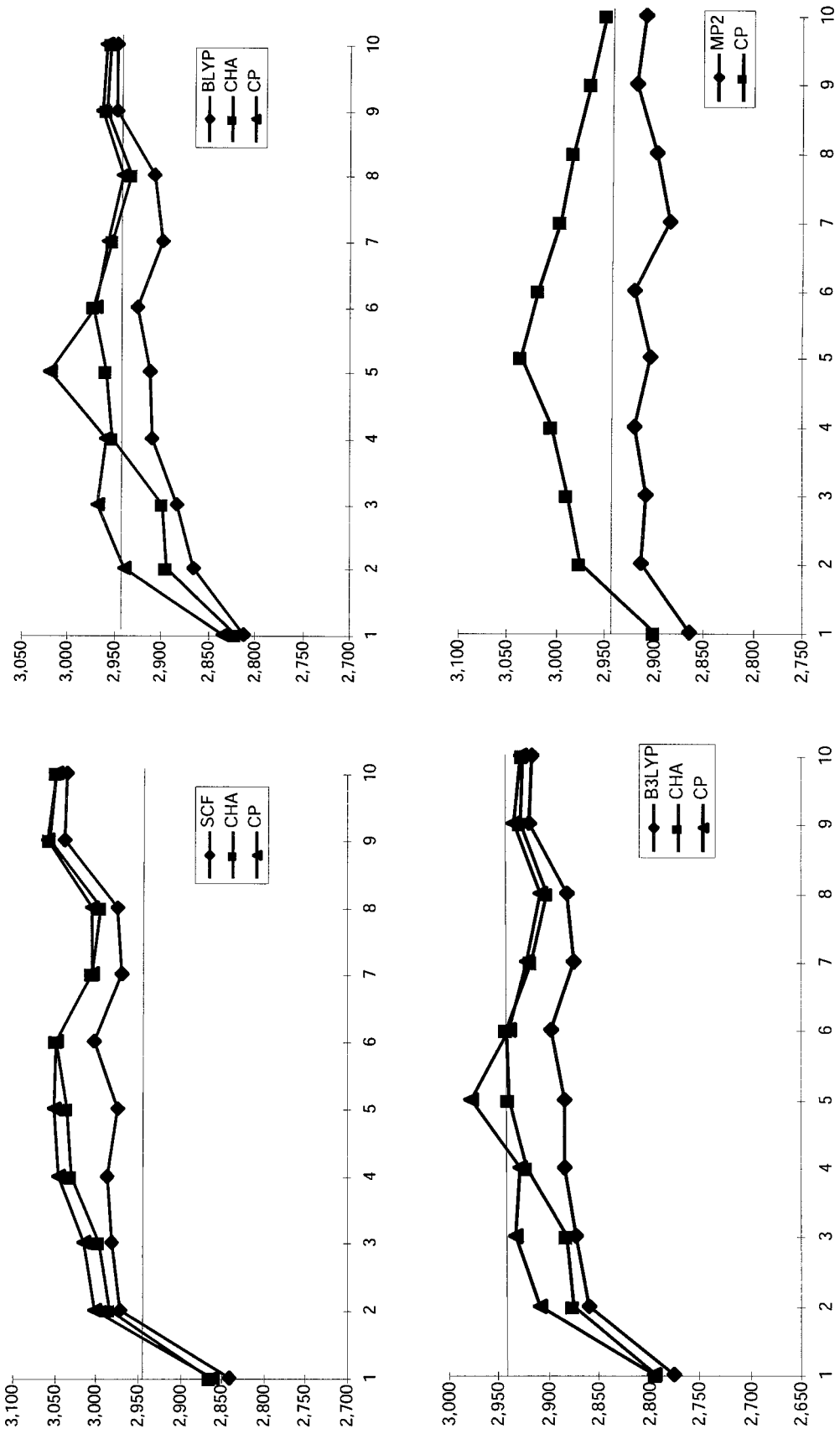

FIGURE 5. Distance between flourine atoms for the complex $(H_2O)_2$ in 10 basis sets. Basis sets are: (1) 6-31G, (2) 6-31G(d), (3) 6-31G(d,p), (4) 6-31++G(d,p), (5) 6-311G(d,p), (6) 6-311++G(d,p), (7) TZV(d,p), (8) TZV++(d,p), (9) 6-311++G(2df,2p), and (10) 6-311++G(3df,2pd). The experimental[31] *roo* distance is ≈2.946 (horizontal solid line).

sponding DFT ones from the PES curvature point of view.

HF–H_2O COMPLEX

The HF–H_2O complex is a rather special system, the determination of its structure is a challenge for both experimentalists and theoretians. Theoretical studies showed[32] that one can find stationary points on the HF–H_2O PES with both C_s and C_{2v} symmetries. [In the case of the C_{2v} structure, the α and β angles (Fig. 1) are 0 and 180 degrees, respectively.] The C_s structure is more stable than the C_{2v} one; the energy difference between them is 0.1 and 0.5 kcal/mol at the SCF and MP2 levels, respectively. The experimental[33] estimate of the barrier is 0.4 kcal/mol. Based on these data one can understand that the experimental determination of the angular features of the HF–H_2O complex is not a trivial task. The barrier is very close to the first vibrational level, most probably the two C_s structures rapidly interconvert to each other and the underlying double well potential can not be measured.

Our main reason for investigating the C_s structure of the HF–H_2O complex was to present a system, which, up to our knowledge, is free from DFT or MP2 pitfalls described in the previous chapters for the cases of the HF and H_2O dimers, respectively. In our opinion, this pitfall-free status of the HF–H_2O complex can be connected with the strength of the interaction in this system. As we go farther from the HF dimer to the H_2O dimer and to the HF–H_2O complex the interaction energies become larger. In the case of the HF dimer the DFT and MP2 methods using small basis sets can totally fail to describe the PES. In the case of the water dimer we found some problems with respect to the curvature of the PES. For the HF–H_2O complex, disregarding the smallest 6-31G basis set, the C_s structure is predicted (Figs 6, 7, Tables V, VI) to be the more stable by all the DFT and MP2 models. In most of the cases when the underlying uncorrected DFT and MP2 methods fail to describe properly the anisotropy of the interaction, the BSSE-corrected α and β angular parameters are close to the large basis results. Concerning the SCF results, one has to mention that in some cases we could find only the C_{2v} structure on the PES. Correction for the BSSE does not change this situation.

Turning to the *rof* geometry parameter, one can draw the following conclusions. Because part of the binding is due to the BSSE, the corrected *rof* distances are always longer than the uncorrected ones. The SCF *rof* distances are nearly always longer than the experimental[34] value of 2.66 Å. Correction for the BSSE further lengthens this parameter. The uncorrected DFT *rof* distances are surprisingly close to the experimental value. In the case of small basis sets, the corrected *rof* distances are farther from the experimental value than the uncorrected ones, but for the largest basis sets they get close to each other. The largest BSSE effects can be found again in the case of the MP2 geometries. The uncorrected *rof* distances usually closer to the experimental value than that of predicted by the CP corrected MP2 model. However, the convergence of the *rof* distance on the corrected PESs is smoother than for the uncorrected PESs.

Comparing the behavior of the CHA and CP correction methods one can find again that differences between both methods are larger in the case of small basis sets. However, if balanced basis sets are used for the calculations both the CP and CHA models perform equally well.

Structures Optimized Using Dunning's aug-cc-pVDZ and aug-cc-pVTZ Basis Sets

The energetical and structural data obtained at the SCF, BLYP, B3LYP, and MP2 levels in conjunction with the Dunning's correlation consistent aug-cc-pVDZ and aug-cc-pVTZ basis sets[35–37,39] on the uncorrected and BSSE-corrected PES, are listed in Tables VII–X.

The correlation consistent [(aug)-cc-p(C)V*X*Z, $X = 2(D), 3(T), 4(Q), \ldots$] basis sets systematically extend the atomic radial and angular spaces as a function of the cardinal numbe *X*. These basis sets were designed to be applied in conjunction with traditional correlation methods where the electron–electron cusp is explicitly described. Because of this feature one expects that the BSSE content of various properties are small using the aug-cc-pVDZ and aug-cc-pVTZ basis sets at the HF and DFT levels. Going further to largest cardinal numbers, the effect of the BSSE on structural and energetical parameters calculated at the HF and DFT levels should decrease enormously. This is not the case, however, for traditional correlation methods like MP2 where the BSSE content of the investigated properties decreases as the cardinal number of the applied basis set is enlarged but it is practically impossible to reach that status when the effect of BSSE becomes negligible. [See, e.g, our recent study[38] on the effect of BSSE on the PESs of small hydrogen-bonded systems studied at the MP2/aug-cc-pV*X*Z ($X = 2, 3, 4, 5$) levels.]

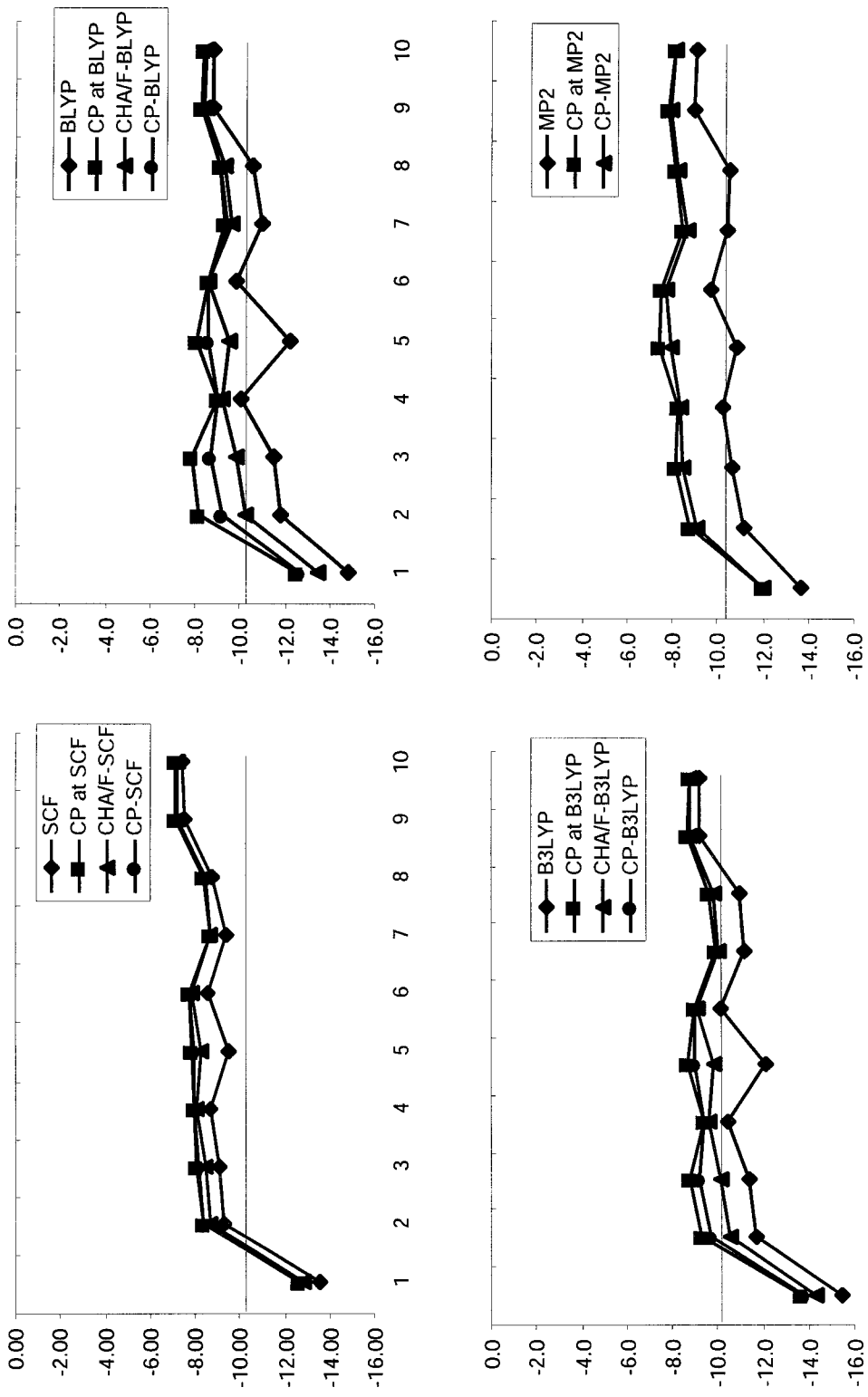

FIGURE 6. Electronic interaction energy (kcal/mol) for the complex HF–H_2O in 10 basis sets. Basis sets are: (1) 6-31G, (2) 6-31G(d), (3) 6-31G(d,p), (4) 6-31++G(d,p), (5) 6-311G(d,p), (6) 6-311++G(d,p), (7) TZV(d,p), (8) TZV++(d,p), (9) 6-311++G(2df,2p), and (10) 6-311++G(3df,2pd). The experimental[37] interactions energy is −10.2 kcal/mol (horizontal solid line).

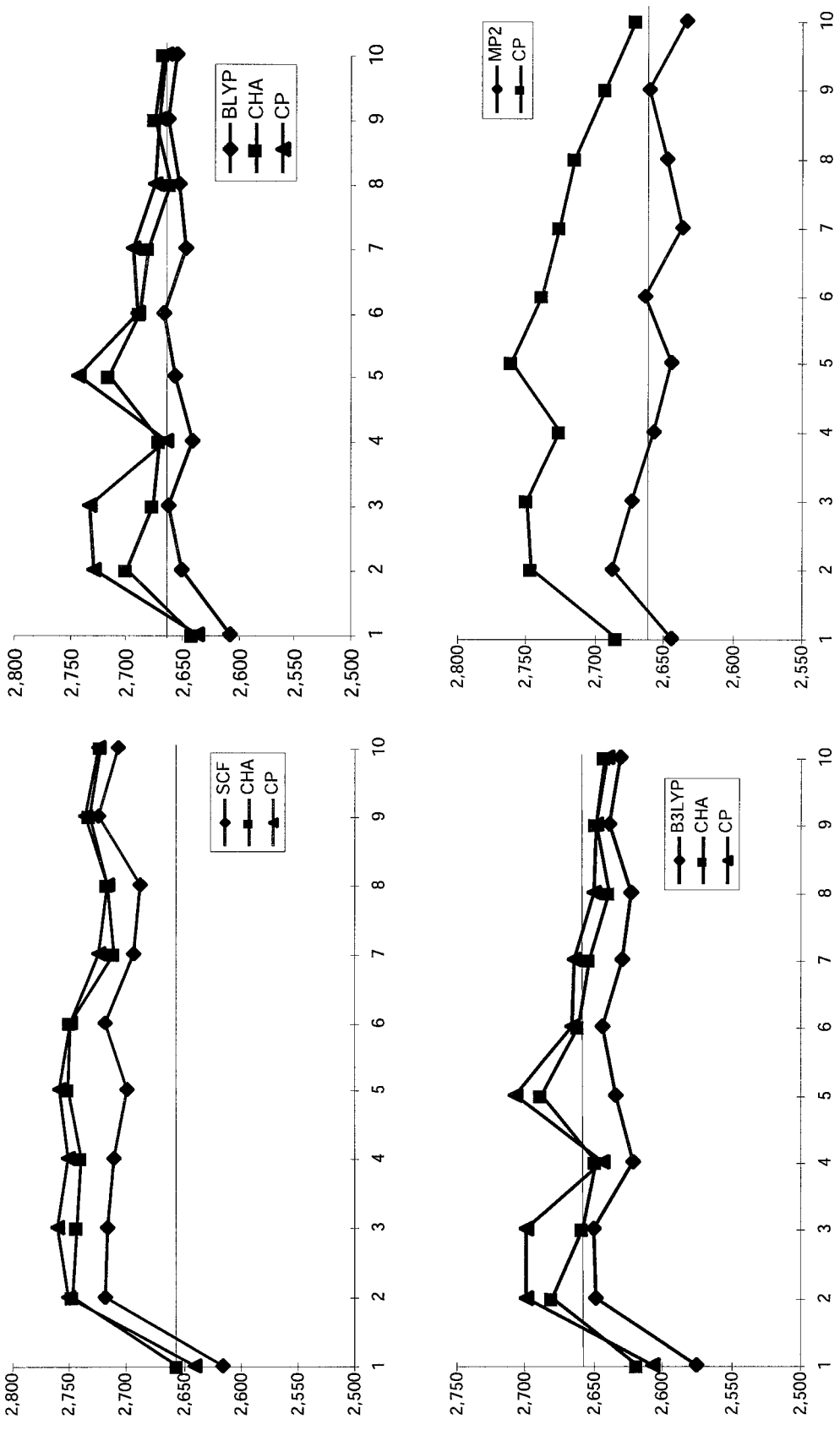

FIGURE 7. Distance between flourine atoms for the complex HF–H_2O in 10 basis sets. Basis sets are: (1) 6-31G, (2) 6-31G(d), (3) 6-31G(d,p), (4) 6-31++G(d,p), (5) 6-311G(d,p), (6) 6-311++G(d,p), (7) TZV(d,p), (8) TZV++(d,p), (9) 6-311++G(2df,2p), and (10) 6-311++G(3df,2pd). The experimental[37] *rfo* distance is ≈2.66 (horizontal solid line).

TABLE V.
Geometrical Parameters for the HF–H_2O Dimer Calculated in 10 Different Basis Sets as the SCF, CHA/F-SCF, CP-SCF, MP2, and CP-MP2 Levels of Theory.

Basis Set	Method	*rfo* (≈)	α	β	Method	*rfo* (≈)	α	β
6-31G	SCF	2.616	0.0	180.0	MP2	2.646	0.0	180.0
(24)	CHA/F-SCF	2.657	0.0	180.0	CP-MP2	2.686	0.0	180.0
	CP-SCF	2.641	0.0	180.0				
6-31G*	SCF	2.719	4.7	132.3	MP2	2.689	7.1	116.9
(36)	CHA/F-SCF	2.749	2.7	140.8	CP-MP2	2.748	2.5	135.8
	CP-SCF	2.753	2.1	146.3				
6-31G**	SCF	2.718	4.0	135.8	MP2	2.675	6.3	117.6
(45)	CHA/F-SCF	2.745	2.2	147.4	CP-MP2	2.750	2.2	135.8
	CP-SCF	2.761	1.7	152.6				
6-31++G**	SCF	2.713	1.6	151.7	MP2	2.659	1.7	138.4
(56)	CHA/F-SCF	2.741	1.1	158.1	CP-MP2	2.727	1.7	140.6
	CP-SCF	2.753	1.1	159.0				
6-311G**	SCF	2.700	2.7	145.4	MP2	2.645	4.1	128.7
(56)	CHA/F-SCF	2.752	0.5	170.9	CP-MP2	2.762	1.0	152.5
	CP-SCF	2.759	0.0	180.0				
6-311++G**	SCF	2.720	0.9	162.5	MP2	2.664	1.4	138.9
(67)	CHA/F-SCF	2.751	0.0	180.0	CP-MP2	2.739	1.4	149.1
	CP-SCF	2.750	0.0	180.0				
TZV**	SCF	2.695	0.0	180.0	MP2	2.637	1.4	146.3
(58)	CHA/F-SCF	2.712	0.0	180.0	CP-MP2	2.727	0.3	172.0
	CP-SCF	2.725	0.0	180.0				
TZV++**	SCF	2.690	0.0	180.0	MP2	2.648	0.9	145.0
(69)	CHA/F-SCF	2.717	0.0	180.0	CP-MP2	2.716	0.8	163.9
	CP-SCF	2.718	0.0	180.0				
6-311++G(2df,2p)	SCF	2.725	1.3	147.0	MP2	2.661	1.3	133.6
(108)	CHA/F-SCF	2.733	1.1	150.6	CP-MP2	2.693	1.4	134.9
	CP-SCF	2.737	1.0	153.7				
6-311++G(3df,2pd)	SCF	2.709	1.2	146.1	MP2	2.635	1.1	134.2
(138)	CHA/F-SCF	2.724	1.1	149.8	CP-MP2	2.671	1.4	133.2
	CP-SCF	2.725	1.1	150.0				

The number of basis functions is given in parentheses. The experimental[34] value of *rfo*(r_0) is ≈2.66. For notation, see Figure 1.

In the light of these facts one can easily rationalize most of our data obtained using these basis sets. All the BSSE-free intermolecular distances are longer than the corresponding uncorrected ones using the aug-cc-pVDZ basis set. However, contrary to the tendency observed for the other basis sets, the CHA distances are slightly longer than the CP ones. The HF and DFT intermolecular distances corrected using the CP method are usually very close to the corresponding uncorrected values (see, e.g., the actual *rfo* values, 2.643 and 2.647 Å (HF–H_2O complex, Table IX) obtained at the B3LYP/aug-cc-pVDZ level on the plain and CP-corrected PESs, respectively. This behavior is a little bit surprising, because the aug-cc-pVDZ basis set is the first and smallest member of the aug-cc-pVXZ family with weaker performance compared to that of the larger (aug-cc-pVTZ, aug-cc-pVQZ, etc.) Dunning basis sets. The CHA distances obtained at the DFT and HF levels seems to be more reasonable in this respect, and are in accordance with the size of the actual basis set.

Our HF and especially the DFT calculations using the aug-cc-pVTZ basis set led to some unexpected results. The difference between the CP-corrected

TABLE VI.

Geometrical Parameters for the HF–H_2O Dimer Calculated in 10 Different Basis Sets as the BLYP, CHA/F-BLYP, CP-BLYP, B3LYP, CHA/F-B3LYP, and CP-B3LYP Levels of Theory.

Basis Set	Method	*rfo* (≈)	α	β	Method	*rfo* (≈)	α	β
6-31G	BLYP	2.610	2.8	149.4	B3LYP	2.576	0.0	180.0
(24)	CHA/F-BLYP	2.642	0.0	180.0	CHA/F-B3LYP	2.619	0.0	180.0
	CP-BLYP	2.638	0.0	180.0	CP-B3LYP	2.608	0.0	180.0
6-31G*	BLYP	2.652	15.2	92.2	B3LYP	2.650	10.4	106.0
(36)	CHA/F-BLYP	2.701	3.3	119.2	CHA/F-B3LYP	2.682	3.2	123.9
	CP-BLYP	2.730	3.2	124.2	CP-B3LYP	2.701	3.0	128.5
6-31G**	BLYP	2.663	13.1	96.2	B3LYP	2.652	8.7	109.5
(45)	CHA/F-BLYP	2.678	3.1	122.1	CHA/F-B3LYP	2.660	3.3	126.1
	CP-BLYP	2.733	2.9	127.3	CP-B3LYP	2.700	2.7	132.4
6-31++G**	BLYP	2.642	2.6	129.4	B3LYP	2.623	2.4	133.8
(56)	CHA/F-BLYP	2.672	2.6	128.9	CHA/F-B3LYP	2.650	2.0	135.4
	CP-BLYP	2.665	2.3	129.3	CP-B3LYP	2.645	2.2	133.9
6-311G**	BLYP	2.657	7.3	113.2	B3LYP	2.636	6.4	119.5
(56)	CHA/F-BLYP	2.716	3.2	126.9	CHA/F-B3LYP	2.690	2.4	135.3
	CP-BLYP	2.744	2.4	135.8	CP-B3LYP	2.708	1.5	145.2
6-311++G**	BLYP	2.668	2.3	132.4	B3LYP	2.645	2.0	137.6
(67)	CHA/F-BLYP	2.689	1.8	133.0	CHA/F-B3LYP	2.663	1.6	139.4
	CP-BLYP	2.691	2.5	131.6	CP-B3LYP	2.667	1.8	141.0
TZV**	BLYP	2.648	2.3	135.3	B3LYP	2.631	1.2	146.4
(58)	CHA/F-BLYP	2.682	1.0	145.8	CHA/F-B3LYP	2.654	1.3	149.1
	CP-BLYP	2.694	1.3	144.4	CP-B3LYP	2.666	1.3	150.8
TZV++**	BLYP	2.654	1.5	138.2	B3LYP	2.625	1.2	146.7
(69)	CHA/F-BLYP	2.662	0.8	143.8	CHA/F-B3LYP	2.640	1.2	148.1
	CP-BLYP	2.675	2.7	136.7	CP-B3LYP	2.652	1.7	146.4
6-311++G(2df,2p)	BLYP	2.664	2.1	127.0	B3LYP	2.640	1.9	131.1
(108)	CHA/F-BLYP	2.675	2.0	126.7	CHA/F-B3LYP	2.650	1.7	131.4
	CP-BLYP	2.672	1.8	127.4	CP-B3LYP	2.650	1.9	131.3
6-311++G(3df,2pd)	BLYP	2.655	1.9	126.5	B3LYP	2.632	1.8	130.9
(138)	CHA/F-BLYP	2.667	1.9	126.8	CHA/F-B3LYP	2.644	1.7	131.4
	CP-BLYP	2.666	1.8	127.5	CP-B3LYP	2.642	1.8	131.1

The number of basis functions is given in parentheses. The experimental[34] value of *rfo*(r_0) is ≈2.66. For notation, see Figure 1.

and the corresponding uncorrected parameters is even smaller (less than 0.006 Å), whereas for three cases (water dimer at the B3LYP/aug-cc-pVTZ and the HF–H_2O complex at the BLYP/aug-cc-pVTZ and B3LYP/aug-cc-pVTZ levels), we could not optimize the geometry of the investigated complexes at the CHA levels. Besides improving our implementation of CHA (application of better convergence accelerators) we tried many numerical tricks to obtain self-consistency of the applied CHA models. For example, the geometry optimizations were started at large intermolecular distances, allowing the optimizer to get slowly close to the particular minimum. At large intermolecular distances the CHA wave functions were easily obtained, but we found serious convergence problems getting close to the desired minima again. In the next step we removed that component of the applied aug-cc-pVTZ basis set that bears the smallest exponent. In this case, our convergence problems disappeared, we could easily obtain optimized geometries using the modified basis set. Somewhat similar problems have been met at small distances by Valiron and Mayer[42] also.

TABLE VII.

Geometrical Parameters for the HF–HF Dimer Calculated Using the aug-cc-pVDZ and aug-cc-pVTZ Basis Sets at the SCF, CHA/F-SCF, CP-SCF, MP2, CP-MP2, BLYP, CHA/F-BLYP, CP-BLYP, B3LYP, CHA/F-B3LYP, and CP-B3LYP Levels of Theory.

Basis Set	Method	*rff*	α	β	Method	*rff*	α	β
aug-cc-pVDZ	SCF	2.826	6.7	118.7	MP2	2.751	6.2	110.6
(68)	CHA/F-SCF	2.854	7.2	119.0	CP-MP2	2.812	6.9	111.6
	CP-SCF	2.846	7.1	118.6				
aug-cc-pVDZ	BLYP	2.761	5.9	109.1	B3LYP	2.734	6.1	110.6
(68)	CHA/F-BLYP	2.805	8.9	107.0	CHA/F-B3LYP	2.774	8.1	109.7
	CP-BLYP	2.772	6.2	109.2	CP-B3LYP	2.745	6.5	110.8
aug-cc-pVTZ	SCF	2.825	6.2	121.0	MP2	2.739	5.5	112.8
(160)	CHA/F-SCF	2.831	6.7	120.2	CP-MP2	2.764	6.6	111.8
	CP-SCF	2.828	6.5	120.4				
aug-cc-pVTZ	BLYP	2.755	5.8	109.9	B3LYP	2.727	6.1	111.4
(160)	CHA/F-BLYP	2.773	4.4	112.7	CHA/F-B3LYP	2.740	5.0	113.6
	CP-BLYP	2.759	6.6	108.7	CP-B3LYP	2.730	6.5	110.8

The number of basis functions is given in parentheses.

In our opinion, the above-described unexpected behavior of the CP and CHA methods, in terms of rather small BSSE and convergence problems, respectively, is related to some fundamental aspects these BSSE-correction models. In both cases one has to specify subsystems of the investigated molecular complexes. This partition is straightforward in the investigated hydrogen bonded complexes, but is clearly not unambiguous when one explores, for example, the effect of BSSE on proton transfer reactions. Another difficulty arises when the applied basis set does consist of basis functions with very small exponents. These functions represent very nonlocal objects, being their assignation to a specific subsystem at least questionable. Indeed, this basis functions could eventually be considered as bond

TABLE VIII.

Geometrical Parameters for the H_2O–H_2O Dimer Calculated Using the aug-cc-pVDZ and aug-cc-pVTZ Basis Sets at the SCF, CHA/F-SCF, CP-SCF, MP2, CP-MP2, BLYP, CHA/F-BLYP, CP-BLYP, B3LYP, CHA/F-B3LYP, and CP-B3LYP Levels of Theory.

Basis Set	Method	*roo*	α	β	Method	*roo*	α	β
aug-cc-pVDZ	SCF	3.037	4.0	130.9	MP2	2.921	6.4	119.6
(86)	CHA/F-SCF	3.062	3.3	132.8	CP-MP2	2.978	5.7	122.5
	CP-SCF	3.053	3.3	133.0				
aug-cc-pVDZ	BLYP	2.950	6.0	118.0	B3LYP	2.920	5.8	120.7
(86)	CHA/F-BLYP	2.995	3.5	126.1	CHA/F-B3LYP	2.961	3.7	127.8
	CP-BLYP	2.958	5.7	119.0	CP-B3LYP	2.929	5.3	122.1
aug-cc-pVTZ	SCF	3.038	2.8	137.7	MP2	2.902	4.7	125.6
(210)	CHA/F-SCF	3.044	3.0	138.0	CP-MP2	2.930	5.4	125.1
	CP-SCF	3.041	2.9	137.9				
aug-cc-pVTZ	BLYP	2.945	5.0	121.0	B3LYP	2.916	4.9	123.8
(210)	CHA/F-BLYP	2.992	8.0	118.0	CHA/F-B3LYP	—	—	—
	CP-BLYP	2.951	5.0	120.3	CP-B3LYP	2.920	5.3	123.5

The number of basis functions is given in parentheses.

TABLE IX.

Geometrical Parameters for the HF–H_2O Dimer Calculated Using the aug-cc-pVDZ and aug-cc-pVTZ Basis Sets at the SCF, CHA/F-SCF, CP-SCF, MP2, CP-MP2, BLYP, CHA/F-BLYP, CP-BLYP, B3LYP, CHA/F-B3LYP, and CP-B3LYP Levels of Theory.

Basis Set	Method	*rfo*	α	β	Method	*rfo*	α	β
aug-cc-pVDZ (77)	SCF	2.725	1.5	142.8	MP2	2.660	1.6	127.7
	CHA/F-SCF	2.760	1.2	149.2	CP-MP2	2.702	1.5	130.3
	CP-SCF	2.734	1.4	144.0				
aug-cc-pVDZ (77)	BLYP	2.664	1.6	126.3	B3LYP	2.643	1.6	130.1
	CHA/F-BLYP	2.684	2.5	128.6	CHA/F-B3LYP	2.664	1.6	135.1
	CP-BLYP	2.668	1.7	126.0	CP-B3LYP	2.647	1.7	129.8
aug-cc-pVTZ (185)	SCF	2.716	1.1	149.5	MP2	2.640	1.3	131.1
	CHA/F-SCF	2.731	1.1	152.3	CP-MP2	2.662	1.4	132.3
	CP-SCF	2.718	1.1	149.8				
aug-cc-pVTZ (185)	BLYP	2.658	1.6	126.4	B3LYP	2.636	1.6	130.9
	CHA/F-BLYP	—	—	—	CHA/F-B3LYP	—	—	—
	CP-BLYP	2.662	1.6	127.1	CP-B3LYP	2.639	1.6	131.2

The number of basis functions is given in parentheses.

functions, therefore not being assigned to any fragment.

The observed behavior of the CP and the CHA methods can be explained on the above basis. The CP approach predicts rather small BSSE content of the investigated properties using the aug-cc-pVDZ basis set. In this case the CHA performs significantly better. However, the observed CHA convergence problems are clearly due to the fact that the investigated minima are located on that region of the PES where, due to the functions with very small exponents present in the basis set, the partition of the whole supermolecule basis set into subsystems is not feasible. This explanation is well supported by the fact that we had no convergence problems at geometries with large intermolecular distances and after removing that basis function of the basis set that bears the smallest exponent. Furthermore, con-

TABLE X.

Uncorrected, CHA/F-Corrected and Counterpoise-Corrected Interaction Energies (kcal/mol) of the HF–HF, H_2O–H_2O, and HF–H_2O Dimers Calculated Using the aug-cc-pVDZ and aug-cc-pVTZ (in Parenthesis) Basis Sets.

HF–HF		H_2O–H_2O		HF–H_2O	
Method	Interaction Energy (kcal/mol)	Method	Interaction Energy (kcal/mol)	Method	Interaction Energy (kcal/mol)
SCF	3.82 (3.72)	SCF	3.86 (3.74)	SCF	7.31 (7.25)
CHA/F-SCF	3.68 (3.65)	CHA/F-SCF	3.71 (3.68)	CHA/F-SCF	6.98 (7.15)
CP-SCF	3.67 (3.65)	CP-SCF	3.71 (3.69)	CP-SCF	7.10 (7.18)
BLYP	4.23 (4.25)	BLYP	4.24 (4.27)	BLYP	8.49 (8.54)
CHA/F-BLYP	3.87 (4.06)	CHA/F-BLYP	3.89 (4.10)	CHA/F-BLYP	7.86 (—)
CP-BLYP	4.04 (4.13)	CP-BLYP	4.06 (4.15)	CP-BLYP	8.26 (8.37)
B3LYP	4.56 (4.56)	B3LYP	4.64 (4.64)	B3LYP	8.89 (8.91)
CHA/F-B3LYP	4.24 (4.41)	CHA/F-B3LYP	4.34 (—)	CHA/F-B3LYP	8.63 (—)
CP-B3LYP	4.38 (4.46)	CP-B3LYP	4.48 (4.53)	CP-B3LYP	8.67 (8.78)
MP2	4.69 (4.76)	MP2	5.24 (5.24)	MP2	8.97 (9.03)
CP-MP2	4.04 (4.27)	CP-MP2	4.45 (4.74)	CP-MP2	7.86 (8.36)

vergence problems were not found in the case of the CHA/F-SCF optimizations where the optimized intermolecular distances are longer than the corresponding CHA/F-DFT values. The same effect can be seen in the case of the BLYP/aug-cc-pVTZ and B3LYP/aug-cc-pVTZ optimizations on the water dimer. The BLYP/aug-cc-pVTZ optimization converged easily, while we had serious convergence problems at the B3LYP/aug-cc-pVTZ level. Analyzing our geometry data it is apparent that the B3LYP intermolecular distances are always shorter than the corresponding BLYP values. One has to note, however, that the validity of the CHA-BLYP/aug-cc-pVTZ geometry for the water is questionable since the BSSE content of dimer distances, the uncorrected *roo* distances (Table VIII) are very similar at the BLYP/aug-cc-pVDZ and BLYP/aug-cc-pVTZ levels predicted by the CHA method. These facts indicate that there is a rather sharp change of behavior of CHA with decreasing intermolecular distances.

Conclusions

In the present article we investigated the effect of the BSSE on the PES and energetics of the $(HF)_2$, $(H_2O)_2$, and HF–H_2O complexes by means of the *a priori* CHA and *a posteriori* Boys–Bernardi BSSE correction methods. One can state that in many of the cases both the CHA/F and CP schemes predict more reliable geometries than those calculated by the corresponding uncorrected methods. As the interaction becomes weaker the BSSE has larger effects on the topology of the PES. In the case of the HF dimer, BSSE contamination can induce drastic changes in the PES resulting cyclic structures for small basis sets. For the water dimer the BSSE can distort the optimized geometry, and the curvature of the surface can be abnormally changed. Finally, for the HF–H_2O complex quite large differences can be observed between the corrected and uncorrected parameters, but the characteristics of the global minimum are left unchanged.

Numerical results show that, in general, CHA/F and CP corrected potential energy surfaces are very similar, and tend to converge to each other as the basis set is improved. Except for a very few cases, the CP method predicts larger interaction energies and longer intermolecular distances than the CHA/F method. However, the moderate and large basis set results clearly show that the CP error compensation scheme can be safely used for the study of intermolecular complexes. The adequacy of the applied basis set can be easily checked by comparing CP and CHA results for the particular problem.

Regarding basis set quality, we can recommend the use of the 6-31++G(d,p), 6-311++G(d,p), TZP(d,p)++, 6-311++G(2df,2p), and 6-311++G(3df,2pd) basis sets in DFT calculations. The use of the the 6-31++G(d,p), 6-311++G(d,p), 6-311++G(2df,2p), and 6-311++G(3df,2pd) basis sets can also be recommended for MP2 calculations. However, attention has always to be paid in the MP2 calculations for the effect of BSSE, because there is no guarantee that whether the BSSE corrected or the underlying uncorrected model behave better compared to experimental results. From this point of view it is worth noting the performance of the MP2/6-31++G(d,p) model. The 6-31++G(d,p) basis set differs only slightly from the 6-31+G(d,p) one, the effect of the diffuse functions on the H atoms cannot be large for the energetics and geometry of the investigated complexes. (On the other hand, most probably, the diffuse functions on the hydrogen atoms increase the BSSE content of the model without representing any significant physical interaction.) As we mentioned in the Introduction, the MP2/6-31+G(d,p) method was successfully applied by Del Bene and coworkers for a wide range of problems despite the deficiences of the model. Analyzing our data one can state that the uncorrected MP2/6-31++G(d,p) model performs well for both the energetics and geometry of the investigated complexes. In many cases the performance of the CP-corrected MP2/6-31++G(d,p) model is worse compared to experiment that that of the uncorrected one. These results suggest again that the MP2/6-31+G(d,p) model could be a good compromise for the study of hydrogen bonded complexes if more sophisticated treatment is prohibited by the size of the investigated system.

Based on our results obtained at the HF and DFT levels in conjunction with the aug-cc-pVDZ and aug-cc-pVTZ basis sets, one can clearly state that the effect of the BSSE on energetical and structural parameters calculated at the above level is not significant. However, despite the fact that there is no practical limitation for the CP method in these cases, the convergence problems that eventually appear with the CHA method indicate that the partitioning of the whole supermolecule basis set including extremely diffuse basis functions, may be conceptually problematic.

As an overall conclusion on the behavior of the CHA and CP correction schemes one can argue that when correction for the BSSE is important both the *a priori* and *a posteriori* methods do the same job at least in a qualitative manner.

Acknowledgments

The authors are indebted to Prof. I. Mayer for valuable discussions on the CHA methods. M.D. and P.S. express their gratitude to the Comission of the European Union for a scholarship, which made their visit to Heidelberg possible.

References

1. (a) Jansen, H. B.; Ross, P. Chem Phys Lett 1969, 3, 140; (b) Boys, S. B.; Bernardi, F. J Mol Phys 1970, 19, 553.
2. Mayer, I.; Surján, P. R. Chem Phys Lett 1992, 191, 497.
3. Valiron, P.; Mayer, I. Chem Phys Lett 1997, 275, 46.
4. Simon, S.; Duran, M.; Dannenberg, J. J. J Chem Phys 1996, 105, 11024.
5. (a) Mayer, I. Int J Quantum Chem 1983, 23, 341; (b) Mayer, I. In Modelling of Structure and Properties of Molecules; Maksic, Z. B., Ed.; Ellis Horwood: Chichester, UK, 1987, p. 145.
6. Mayer, I. Int J Quantum Chem J Chem Phys 1998, 70, 41.
7. Paizs, B.; Mayer, I. Chem Phys Lett 1994, 220, 97.
8. Pople, J. A.; Krishnan, R.; Schlegel, H. B.; Binkley, J. S. Int J Quantum Chem Symp 1979, 13, 225.
9. Paizs, B. Ph. D. thesis, Eötvös Loránd University, Budapest (1996).
10. Handy, N. C.; Schaefer, H. F., III J Chem Phys 1984, 81, 5031.
11. Helgaker, T.; Jorgensen, P. Theoret Chim Acta 1989, 75, 111.
12. Mayer, I.; Valiron, P. J Chem Phys 1998, 109, 3360.
13. Del Bene, J. E.; Person, W. B.; Szczepaniak, K. J Phys Chem 1995, 99, 10705, and references therein.
14. As the strength of the hydrogen bond decreases the role of dispersion becomes more important in the interaction. Because the present DFT functionals are not capable to describe dispersion forces,[15, 16] DFT methods fail to predict reasonable parameters for the case of weakly bonded systems.[17]
15. Kristyán, S.; Pulay, P. Chem Phys Lett 1994, 229, 175.
16. Pérez-Jordá, J. M.; Becke, A. D. Chem Phys Lett 1995, 233, 134.
17. Paizs, B.; Suhai, S. J Comput Chem 1997, 19, 575.
18. Frisch, M. J.; Trucks, G. W.; Head-Gordon, M.; Gill, P. M. W.; Wong, M. W.; Foresman, J. B.; Johnson, B. G.; Schlegel, H. B.; Robb, M. A.; Replogle, E. S.; Gomperts, R.; Andres, J. L.; Raghavachari, K.; Binkley, J. S.; Gonzalez, C.; Martin, R. L.; Fox, D. J.; Defrees, D. J.; Baker, J.; Stewart, J. J. P.; Pople, J. A. Gaussian Inc.: Pittsburgh, PA, 1992.
19. Frisch, M. J.; Trucks, G. W.; Schlegel, H. B.; Gill, P. M. W.; Johnson, B. G.; Robb, M. A.; Cheeseman, J. R.; Keith, T. A.; Petersson, G. A.; Montgomery, J. A.; Raghavachari, K.; Al-Laham, M. A.; Zakrzewski, V. G.; Ortiz, J. V.; Foresman, J. B.; Cioslowski, J.; Stefanov, B. B.; Nanayakkara, A.; Challacombe, A.; Peng, C. Y.; Ayala, P. Y.; Chen, W.; Wong, M. W.; Andres, J. L.; Replogle, E. S.; Gomperts, R.; Martin, R. L.; Fox, D. J.; Binkley, J. S.; Defrees, D. J.; Baker, J.; Stewart, J. J. P.; Head-Gordon, M.; Gonzalez, C.; Pople, J. A. Gaussian Inc.: Pittsburgh, PA, 1995.
20. Paizs, B.; Suhai, S. J Comput Chem 1997, 18, 695.
21. Becke, A. D. Phys Rev A 1988, 38, 3098.
22. Lee, C.; Yang, W.; Parr, R. G. Phys Rev B 1988, 37, 785.
23. Becke, A. D. J Chem Phys 1993, 98, 5640.
24. Howard, B. J.; Dyke, T. R.; Klemperer, W. J Chem Phys 1984, 81, 5417.
25. Mayer, I.; Túri, U. J Mol Struct (Theochem) 1991, 227, 43.
26. Maerker, C.; Schleyer, P. v. R.; Liedl, K. R.; Ha, T.-K.; Quack, M.; Suhm, M. A. J Comput Chem 1997, 18, 1695, and references therein.
27. Hobza, P.; Sponer, J.; Reschel, T. J Comput Chem 1995, 11, 1315.
28. Pine, A. S.; Howard, B. J. J Chem Phys 1983, 84, 590.
29. Odutola, J. A.; Dyke, T. R. J Chem Phys 1980, 72, 5062.
30. Halkier, A.; Koch, H.; Jorgensen, P.; Christianses, O.; Beck Nielsen, I. M.; Helgaker, T. Theor Chem Acc 1997, 97, 150, and references therein.
31. Reimers, J.; Watts, R.; Klein, M. J Chem Phys 1982, 64, 95.
32. Szczesniak, M. M.; Scheiner, S.; Bouteiler, Y. J Chem Phys 1984, 81, 5024.
33. Legon, A. C.; Millen, D. J. Faraday Discuss Chem Soc 1982, 73, 71.
34. Legon, A. C.; Millen, D. J.; North, J. M. Chem Phys Lett 1987, 135, 303.
35. Dunning, T. H., Jr. J Chem Phys 1989, 90, 1007.
36. Kendall, R. A.; Dunning, T. H., Jr.; Harrison, R. J. J Chem Phys 1992, 96, 6796.
37. Woon, D. E.; Dunning, T. H., Jr. J Chem Phys 1993, 98, 1358.
38. Paizs, B.; Salvador, P.; Császár, A. G.; Duran, M.; Suhai, S., submitted for publication.
39. Peterson, K. A.; Dunning, T. H., Jr. J Chem Phys 1995, 102, 2032.
40. Feller, D.; Glendening, E. D.; Kendall, R. A.; Peterson, K. A. J Chem Phys 1994, 100, 4981.
41. Xantheas, S. S. J Chem Phys 1996, 104, 8821.
42. Mayer, I., private communication.